13th ewtec 2019 Proceedings of the 13th European Wave and Tidal Energy Conference 1-6 Sept 2019, Naples, Italy

Full- and model scale Testing of two different Rotor Diameters for Instream Power Generation

Ralf Starzmann, Nicholas Kaufmann and Penny Jeffcoate

Abstract—**As the tidal energy sector starts to move from demonstration towards first commercial projects a key focus is on reducing the costs. In order to standardize the turbine system SCHOTTEL HYDRO have developed their current commercial 4m SCHOTTEL Instream Turbines (SIT), as well as larger 6.3m diameter rotors which use the same SIT250 drivetrain. The larger rotor diameter is suited to lower flow speed sites, whereas the smaller rotor dimeter is suited for higher resource sites. Four SIT250 drivetrains of both rotor diameters can be deployed to the surface platform PLAT-I by Sustainable Marine Energy. The system has undergone sea testing using the 4m rotors between November 2017 and June 2018 in the UK, and is now deployed in Nova Scotia (Canada) since September 2018 with 6.3m rotors. This paper presents the hydrodynamic rotor performance and its comparison for both rotor sizes including model scale and full-scale experimental results. The objective is to demonstrate the principle performance of both rotor geometries and compare hydrodynamic properties of the two designs.**

The performance for both rotors shows good agreement with semi-empirical performance predictions. In general, the results derived from the testing provide a high level of design confidence in the turbines' performance.

Keywords— **Full-Scale Testing, Model Scale Testing, SIT 250, Tidal Turbine.**

I. Introduction

THE development of rotor blades for a horizontal axis instream turbine is a stepwise, iterative process. It includes design, numerical simulation, testing and validation of both the hydrodynamic and structural design and often involves iterations [1]. Solely focusing on the hydrodynamic performance, the following three steps are crucial:

- Hydrodynamic design
- Model scale testing
- Full-scale field testing.

During the hydrodynamic design the overall turbine design philosophy plays an important role. Both variable pitch [2] and fixed pitch [3] turbines are currently used in the tidal sector. In the case of fixed pitch turbines, the turbine control philosophy, e.g. stall regulated or overspeed regulated [4], as well as the positioning in the water column must be considered. Aside from the hydrodynamic efficiency, thrust behaviour and cavitation inception are important design objectives. Blade element momentum (BEM) [6] [7] [8] [9] as well as computational fluid dynamics (CFD) [10] methods are used during the design phase.

Throughout the development of hydrokinetic turbines, towing tanks as well as flumes have been used for model scale testing; see e.g. [11], [12] and [13]. Standardisation work is underway from both the International Electrical Commission (IEC) [14] and the International Towing Tank Conference (ITTC) [15] but not yet in a similar standard as used for traditional propeller testing.

For full-scale operational tests guidelines and test methodology are set out in IEC62600-200, the technical specification for Tidal Energy Converter (TEC) power performance assessment [16]; this standard has been used previously to assess the performance of seabed mounted [17] as well as floating tidal turbines [18] [19].

This paper presents measured performance characteristics of a horizontal axis free-flow turbine utilizing two different rotor sizes, 4m diameter and 6.3m diameter. The experimental results are obtained in model scale towing tank tests as well as in full-scale field tests. The overall objectives of this work are:

- To demonstrate turbine characteristics (power & thrust) using model scale testing in a towing tank following the ITTC standards
- Demonstrate full scale power performance assessment of the individual rotors according to IEC/TS 62600-200
- Compare the performance of both rotors.

ID number: 137710-30 and conference track: TDD.

This work been funded by the Federal Ministry for Economic Affairs and Energy of Germany (BMWi) in the project TIDAL POWER (FKZ 0325817B)

R. Starzmann is with SCHOTTEL HYDRO, Mainzer Straße 99, 56321 Spay/Rhine, Germany (e-mail: rstarzmann@schottel.de).

N. Kaufmann was at the Institute for Fluid- and Thermodynamics, University of Siegen, 57068 Siegen, Germany, he is now with SCHOTTEL HYDRO Mainzer Straße 99, 56321 Spay/Rhine, Germany (e-mail: nkaufmann@schottel.de).

P. Jeffcoate is with Sustainable Marine Energy, La Belle Esperance, The Shore, Edinburgh, UK (e-mail: penny.jeffcoate@sustainablemarine.com).

II. SCHOTTEL INSTREAM TURBINE

A. Development History

SCHOTTEL HYDRO's SCHOTTEL Instream Turbine (SIT 250) is a horizontal axis free-flow turbine. The first generation SIT 250 was presented by SCHOTTEL in 2012, as shown on in Fig 1 (a) [20]. Comprehensive testing has been carried out and published for the first generation turbine using a 4m rotor. These include full-scale pushing tests in Rotterdam harbour [20] and moored tests using a floating platform at Queen's University Belfast's Tidal Test Site in Strangford Lough [18]. A comparison of both data sets showed comparable power output and performance curves for both the steady and turbulent tidal tests [21]. Model test data collected in a towing tank setup overall correlated very well with the full-scale performance data [22]. Furthermore, a comparison with respect to cavitation inception using model-scale and full-scale experiments showed reasonable agreement with a semi empirical model [9] .

(a) (b)

Fig. 1 SCHOTTEL Instream Turbine - SIT 250 (4m rotor diameter; (a): 1st generation, (b): 2nd generation)

Performance prediction using BEM has been validated for the second generation SIT 250 ((b) in Fig 1) blade geometry using a 4m rotor [19]. This included model scale towing tank as well as cavitation tunnel data and showed very good agreement for power and thrust coefficients, as well as the cavitation inception bucket over a wide range of tip speed ratios [9]. The full-scale turbine was also tested on Sustainable Marine Energy's surface floating PLAT-I platform and showed good agreement with semi-empirical power and thrust predictions using BEM [19].

B. Modular Turbine System

The SIT 250 is designed as a modular turbine system utilizing one drivetrain for two rotor diameters, 4 m and 6.3 m, which can be selected based upon the varying velocity frequency distributions of different deployment sites.

Ideally, the turbine rotor design would be optimized for the velocity frequency distribution of a specific site where the installation is planned. Given the present techniques of blade manufacture, this is not cost-effective. Hence, the rotor designs are tailored for two generic tidal current velocity distributions: one suitable for a higher (class I) and the other a lower (class II) energy site. The chosen distributions are believed to cover the demands of a large number of prospective sites. The annual hours of occurrence based on the generic velocity frequency distributions are shown in Fig. 2.

The SIT 250 drive train is rated at the mechanical shaft, so rated power and grid-ready electrical power are P_{rated} = 85 kW and P_{el} = 70 kW respectively. Both three-bladed rotor versions are manufactured from composite material to provide passive-adaptive pitch behaviour. The blades are fitted onto a standardized hub with a diameter of 0.36 m. This unavoidably leads to different hub-to-tip diameter ratios for the chosen rotor sizes and thus demands a unique design for both diameters. A simple up-scaling is not possible. A rotor hub, a slow speed shaft, a planetary gearbox and asynchronous generator complete the drive train; the system is cooled by ambient water. The BEM predicted power curves of the two rotor configurations are compared in Fig. 3.

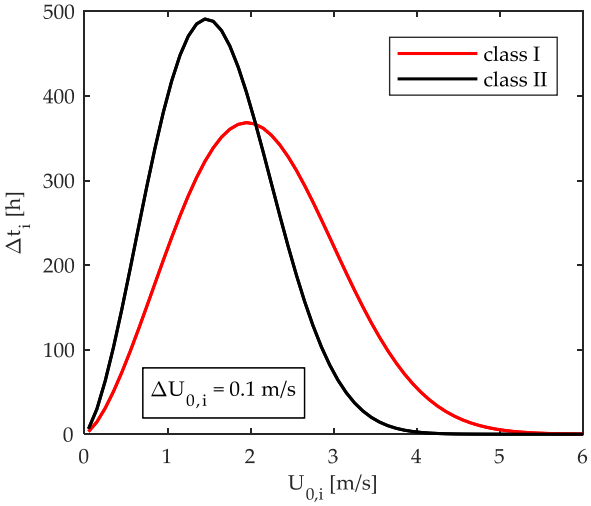

Fig. 2 Specified generic velocity frequency distributions used for the turbine design (SCHOTTEL class system).

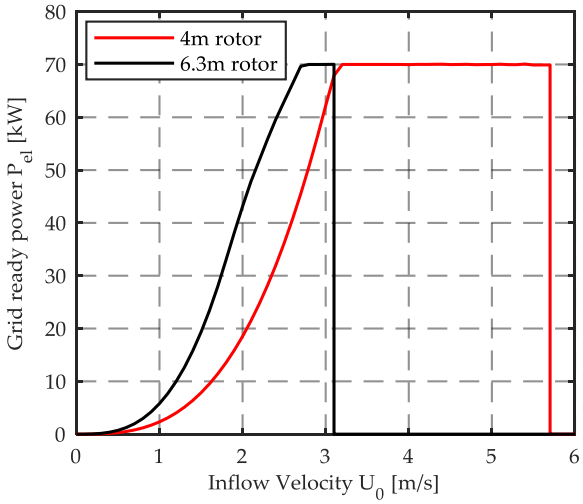

Fig. 3 Electrical power output as function of the undisturbed inflow velocity far upstream.

Special attention was given to the hydrodynamic design of the turbine blades. A novel multi-objective optimizing scheme, described in [6], has been developed

targeting the best compromise between maximum power output, minimum thrust load and shallowest immersion depth for operation without cavitation. Table I summarizes the properties of the modular turbine system.

TABLE I
SIT 250 MODULAR TURBINE SYSTEM

P_{rated}	rated power (mechanical)	85 kW	
P_{el}	rated power (grid ready)	70 kW	
-	pitch control	none (fixed-pitch)	
-	variable speed control	yes	
d_{hub}	hub diameter	0.36 m	
d_{tip}	rotor diameter	4 m	6.3 m
λ_D	design tip speed ratio	5	6
$C_P(\lambda_D)$	power coefficient at the design point (rigid blade)	0.45	0.46
$C_T(\lambda_D)$	thrust coefficient at the design point (rigid blade)	0.80	0.75

C. PLAT-I Floating Platform

PLAT-I is a three-hulled tidal energy platform that hosts four SIT 250 turbines. The turbines are suspended from the cross-deck, via lifting support structures called SIT Deployment Modules (SDMs). During normal operation, or when parked, the turbines are in the down configuration, but they can be lifted clear of the water for maintenance, Fig. 4.

Fig. 4 SIT 250s (4m blades) and SDMs in maintenance position in Connel (November 2017)

The platform self-aligns to incoming flow via a mooring turret, which is connected to a geostationary mooring spread. Fig. 5 shows the platform in operation at the Falls of Lora in Connel, whereas Fig. 6 shows the platform during blade install in Grand Passage.

Fig. 5 PLAT-I in operation as deployed in Connel, Oban (4 m rotors)

Fig. 6 Blade installation (6.3m rotors) in Grand Passage (February 2019)

The turbines operate in both clockwise and counter-clockwise direction (looking upstream), as shown in Fig. 7. The turbines are named SIT1 to SIT4 from Port to Starboard, Fig. 7. The hub deployment depth is 4.7m.

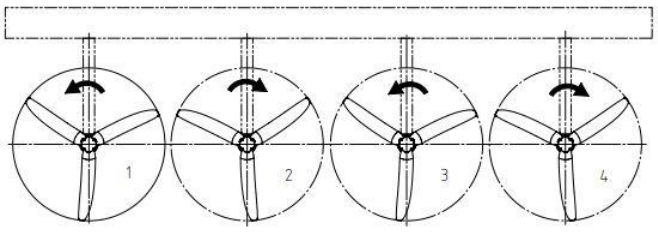

Fig. 7 Schematic SIT 250 configuration on PLAT-I

III. EXPERIMENTAL SETUP

The testing methodology is presented below for both the model scale as well as for the full-scale setup.

D. Model Scale Testing

All model scale experiments were performed at the Schiffbau-Versuchsanstalt Potsdam GmbH (SVA). SVA was commissioned to manufacture the turbine rotors, manufacture the dummy housing and perform the tests.

The 1:8 and 1:12.6 scale size, respectively, was selected in accordance to Reynolds number effects and cavitation inception threshold over the predetermined inflow velocity.

Tests were carried out at various different velocities, whereas only results for $U_0 = 2$ m/s are presented in this study. For the towing tank experiments, trials were performed at a depth of 0.5m; this position was selected in accordance to traditional propeller testing (ITTC) - positioning the centre of the rotor shaft 1 turbine diameter below the waterline. The turbine was fixed to a dynamometer. The rotor shaft was located downstream of the rotor, shown in Fig. 8 [30]. The cross-sectional blockage of the open water tests was 0.5%. The most relevant data of the towing tank are compiled in Table II.

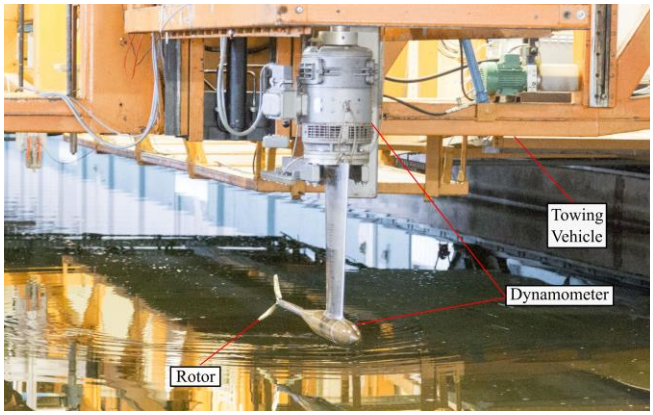

Fig. 8 SVA towing tank setup [30].

TABLE II
SVA TOWING TANK TEST FACILITY

Towing tank dimensions	280.0 m length 9.0 m width/breadth 4.5 m depth
Maximum carriage velocity	7.0 m/s
Dynamometer H39	nmax=60s-1 Tmax=1000N Qmax=50Nm
Immersion of Rotor shaft	0.5m
Model rotor diameter	0.5m (1:8 and 1:12.6 scale)
Material of model rotor	Brass

E. Field Testing

Full-scale field testing using the PLAT-I platform was carried out at two different deployment sites, the Falls of Lora in Scotland (UK) and Grand Passage in Nova Scotia (Canada).

1) Falls of Lora (Connel/Scotland)

The platform was installed downstream from the Falls of Lora between November 2017 and June 2018. Many different test configurations and operational parameters were assessed during the field tests, see [19] [24]. The test site is located at Connel at the mouth of Loch Etive in Scotland. This is a sheltered sea loch with a large tidal zone, creating strong flows but minimal wave conditions. The site is only exposed to the West, but surrounding coast and islands reduce the fetch and therefore wave climate. The flow speed on the ebb is driven by a jet formed by the Falls of Lora. This gives a strong localised flow with high temporal and spatial variation, but with calm surrounding conditions for access and support infrastructure. Additionally, the flood tide is very benign, giving long operational windows for maintenance.

2) Grand Passage (Westport/Nova Scotia)

The platform was relocated from Scotland during summer 2018, to Grand Passage at the southern tip of Digby neck in September 2018. Digby Neck is a strip of land located at the mouth of the Bay of Fundy in Nova Scotia, Canada. Three channels – Grand Passage, Petit Passage and Digby Gut – cut through the Neck and have been deemed suitable for tidal power extraction [25]. Grand Passage is the westernmost of the three passages. It separates Brier Island to the west from Long Island to the east. The flood tide runs south to north through Grand Passage. In the middle of the channel there is only a small directional asymmetry in the flow and the current magnitudes on the flood and ebb tides are nearly symmetric [25]. In general the site is much more exposed with respect to waves compared to Connel, though it is still a sheltered site. A number of detailed site investigations including numerical and experimental work have been carried out to characterize the tidal resource in Grand Passage [26][27][28].

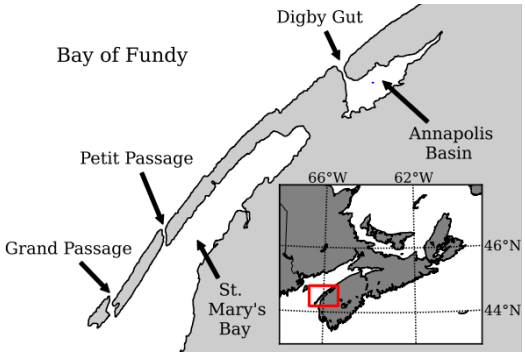

Fig. 9 Digby Neck region [25]

3) Instrumentation

Instruments were mounted on the platform to measure the current velocity, turbine performance and reaction force at the SDM (due to rotor thrust and SDM drag). These are detailed in Table III and Fig. 10. The rotor thrust was derived by resolving the forces acting on the SDM, including SDM drag, SDM and SIT masses, and rotor thrust, see [24] for more details.

The IEC standard [14] defines a bed mounted current profiler (ADCP) as the preferred current velocity measurement device, as well its postion relative to the energy extraction plane. However, since the platform swings

with the flow direction, in this work a Valeport Electromagentic Current Meter (ECM) close to the water surface is used. The ECM only provides a single measurement point, rather than a power-weighted average of the flow at hub height as derived from a flow profile as per IEC recommendation. Though this does not comply with IEC recommendation the IEC method will be followed where possible to validate performance.

TABLE III
TEST INSTRUMENTATION

Parameter	Instrument	Location	Label
Power	S120 SIEMENS Inverter	Control Container	3
Torque	S120 SIEMENS Inverter	Control Container	3
Rot. Speed	S120 SIEMENS Inverter	Control Container	3
Velocity	Valeport Electromagnetic Current Meter	Connel - Upstream from SIT2 6.1m, 27cm below water surface GP - Upstream from SIT3, 6.1m, 27cm below water	2
Reaction force at pins (Thrust)	LCM Load Pin	Lower connection point between SDM and crossdeck structure	1

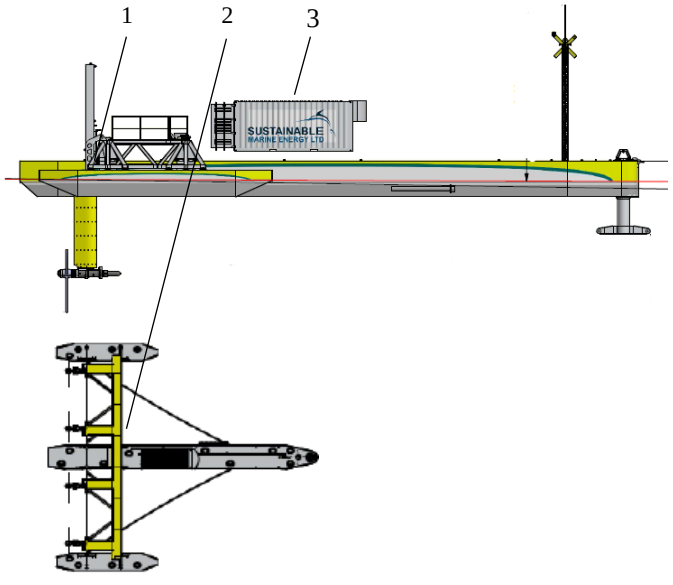

Fig. 10 PLAT-I with instrumentation locations (side and top view)

IV. DATA PROCESSING

F. Post-Processing Model Scale Testing

Open water tests were carried out over a range of tip speed ratios. The variation in TSR was achieved by varying the rotational speed for a given inflow speed. Measured values of thrust, torque, rotational speed and inflow speed were recorded together, with time series, maximum and minimum values and standard deviations of the signals. According to the recommendations of the International Towing Tank Conference (ITTC), the measured values for thrust and torque were corrected using the values obtained for the dummy hub of the same mass of the model turbine. Drag was corrected with zero coefficients from the streamlined hubcap. Torque was corrected for the effect of frictional values of torque, taken with the shaft rotating at the same speed with an axis symmetric mass.

G. Post-Processing Field Testing

Various sampling rates had been used during the data collection for different instruments and test objectives, however all data in this work was reduced to 1Hz. All data was recorded synchronously and no filtering was applied to the data sets. All post-processing was applied to the data as per IEC [14]. Further detail and equations can be found in the reference document, though key equations will be presented here. The IEC suggests using an averaging period between 2 and 10 min; the data presented here has been 2 min averaged. In general, the following steps are performed using the bin methodology:

1. Calculate the mean recorded current velocity u of a 2 min data set, as per equation 2, where i is the flow velocity bin, j is the instantaneous velocity data point, L is the number of instantaneous velocity data points, and n is the number of data points in a velocity bin.

$$\bar{U}_{i,n} = \left[\frac{1}{L} \sum_{j=1}^{L} \hat{U}_{i,j,n}{}^{3} \right]^{1/3} \quad (1)$$

2. Calculate mean value of the respective data sources (e.g. power, thrust, rot. speed)
3. Sort these values into the corresponding flow velocity bins
4. Calculate mean value for each flow velocity bin, i.
5. Sort the time averaged data into operating (producing power), free-wheeling, or parked (brake applied).

Mean bin equations for velocity u, electrical power P_{el}, thrust T, torque M and rotational speed n are given below. Each bin increment was chosen as 0.05 m/s.

$$\bar{U}_i = \frac{1}{N_i} \sum_{n=1}^{N_i} \bar{U}_{i,n} \quad (2)$$

$$\bar{P}_{el,i} = \frac{1}{N_i}\sum_{n=1}^{N_i} \bar{P}_{el,i,n} \tag{3}$$

$$\bar{T}_i = \frac{1}{N_i}\sum_{n=1}^{N_i} \bar{T}_{i,n} \tag{4}$$

$$\bar{M}_i = \frac{1}{N_i}\sum_{n=1}^{N_i} \bar{M}_{i,n} \tag{5}$$

$$\bar{n}_i = \frac{1}{N_i}\sum_{n=1}^{N_i} \bar{n}_{i,n} \tag{6}$$

As per IEC the water-to-wire efficiency is defined as

$$\eta_{System,i} = \frac{\bar{P}_{el,i}}{\frac{1}{2}\rho A \bar{U}_i^3} \tag{7}$$

The mechanical power, P_m, is derived from equation 8 using a drive train and electrical system efficiency. With that the power coefficient c_p is calculated. A constant water density of ρ = 1025 kg/m³ was used. The area, A, is the swept area of the rotor.

$$P_m = \frac{\bar{P}_{el,i}}{\eta_{drivetrain}\eta_{el\ system}} \tag{8}$$

$$c_P = \frac{P_{mech}}{\frac{1}{2}\rho A \bar{U}_i^3} \tag{9}$$

The thrust coefficient, c_T, is also calculated using the thrust, T, and the same parameters as the power coefficient calculation. The tip speed ratio, λ, is determined using the inflow velocity, angular velocity, ω, and rotor radius, R.

$$c_T = \frac{\bar{T}_i}{\frac{1}{2}\rho A \bar{U}_i^2} \mathrm{P_{flow}} = \frac{1}{2}\rho \mathrm{AU}^3 \tag{10}$$

$$\lambda = \frac{\omega R}{\bar{U}_i} \mathrm{P_{flow}} = \frac{1}{2}\rho \mathrm{AU}^3 \tag{11}$$

The thrust is calculated from the reaction force at the SIT Deployment Module (SDM) connection. This is determined from the force balance resolved about the SDM hinge point. The calculated force includes drag on the structure and rotor and so is denoted F_x, force in the axial, x, direction.

Velocity fluctuations are quantified in terms of turbulence intensity, *TI*. This is defined as the fluctuating part of the velocity divided by the mean velocity: The turbulence intensity at the current meter for each data set within each velocity bin was calculated.

$$TI = \frac{U_i'}{\bar{U}_i} \mathrm{P_{flow}} = \frac{1}{2}\rho \mathrm{AU}^3 . \tag{12}$$

V. RESULTS

H. Model Scale testing

The experimental results obtained in the towing tank of the scaled models of the 4 m and 6.3 m rotor are shown in Fig. 11. The measurements were conducted at an inflow velocity of U_0 = 2 m/s. Recall, the rotor diameter of both model turbines is D = 0.5 m leading to different scaling factors of 1:8 (4 m rotor) and 1:12.6 (6.3 m). Thus, the local Reynolds numbers of the 6.3 m rotor are below the values of the 4 m turbine. The C_P of the 4 m rotor is slightly above the 6.3 m rotor for the interesting tips speed ratio range $\lambda \geq \lambda_{opt}$. This is due to the lower Reynolds number for the 6.3m rotor model. However, the thrust coefficient of the 6.3m rotor is distinctively reduced for a wide operating range (cp. diagram (b)) as compared to the 4 m rotor. Summarizing, the similar C_P values and the lower C_T values of the 6.3 m rotor lead to a favourable power to thrust ratio as shown in Fig. 11 (c).

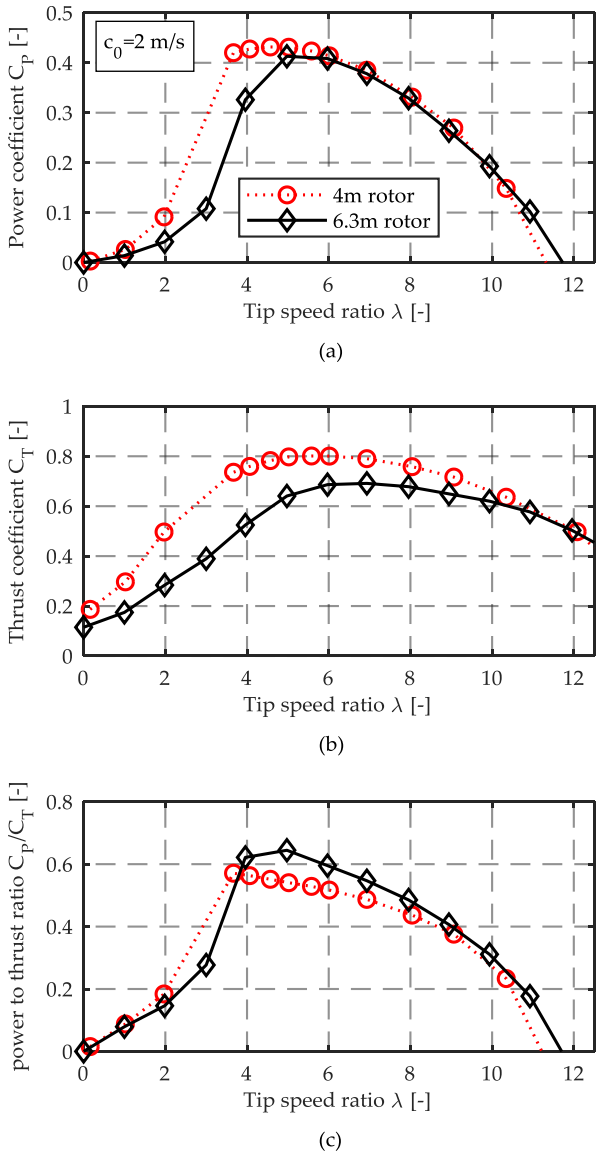

Fig. 11 Towing tank tests of the 0.5 m diameter model scale turbines: (a) power coefficient; (b) thrust coefficient and (c) power to thrust ratio as function of the tip speed ratio

I. Field Testing of the Full-Scale Turbines

As mentioned above, the two rotors were tested at the same drivetrains and platform but at two different test sites. The average turbulence intensity *TI* is compared for the two test sites in Fig. 12. The presented *TI* is based on the data sets used for the performance assessment discussed below. The flow conditions at the test site at Connel (4 m rotor) are considerably more turbulent as compared to the current demonstration site at Grand Passage (6.3 m rotor). The *TI* at Connel is around 30% whereas it converges at around 10% for Grand Passage. This emphasises the special conditions in the wake of the Falls of Lora and quantifies the high temporal variation in flow that the turbines are operating in. Within the limited testing time at Grand Passage so far, the two minute averages of the inflow velocity reaches a maximum of 2.2 m/s.

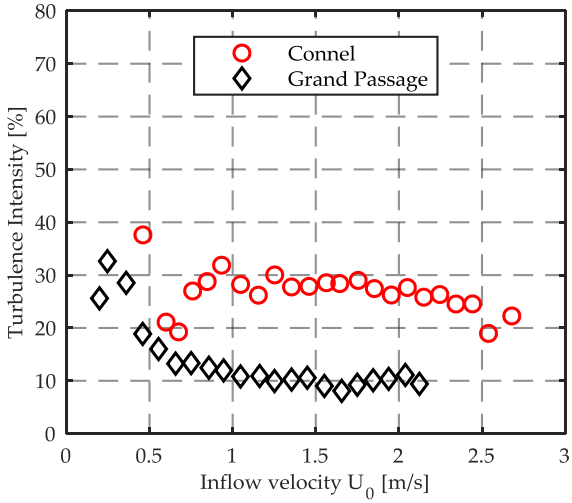

Fig. 12 Comparison of the mean turbulence intensity for the test sites in Connel, Scotland (4 m turbine) and Grand Passage, Canada (6.3 m turbine)

The power curves, obtained following the IEC procedure, are shown in Fig. 12 for the 4 m and 6.3 m rotor, respectively. Attributed to the larger swept area, the power curve of the 6.3 m version provides significantly higher power compared to the 4 m rotor. Thus, the 6.3 m rotor provides a higher power output up to P_{rated}. However, neither for the 4m rotor nor for the 6.3m rotor the flow speed data sets as used in this study were sufficient to reach rated power. Since flow speeds in Grand Passage do exceed $U_0 = 3.0$ m/s a wider range of the power curve will be available soon.

Besides the measuring results, the BEM-predicted power curves are presented. Since the power is taken at the input of the inverter, the losses within the drive train are considered. The agreement between prediction and experimental data is very satisfactory for both cases. Nevertheless, the power output of the 6.3 m rotor is slightly underpredicted.

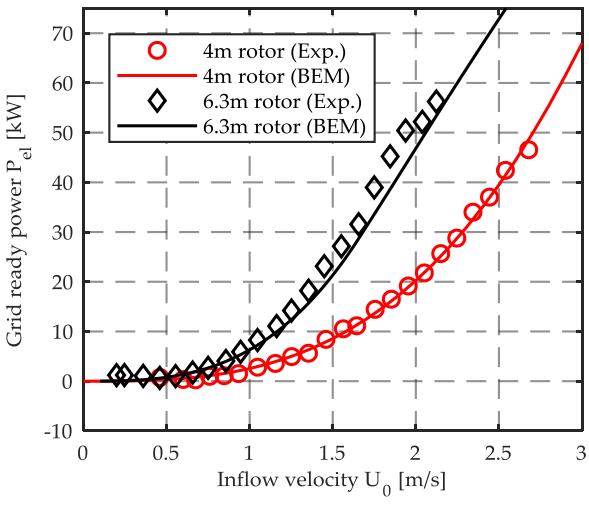

Fig. 13 Comparison of predicted and measured turbine power as function of the inflow velocity for the 4 m rotor and the 6.3 m rotor, respectively

The thrust curves based on the load pin measurements at the SDMs are presented in Fig. 14 for both rotors. As for the power, the thrust of the 6.3 m rotor is significantly above the values of the 4 m rotor as a result of the larger diameter. Thus, in return of the higher power output of 6.3 m rotor the loads on the platform and the anchoring are increased. The BEM simulations underpredict the measured thrust for both rotors. To a certain degree, this is because the drag of the SDM and nacelle, though very low, are included in the measured data.

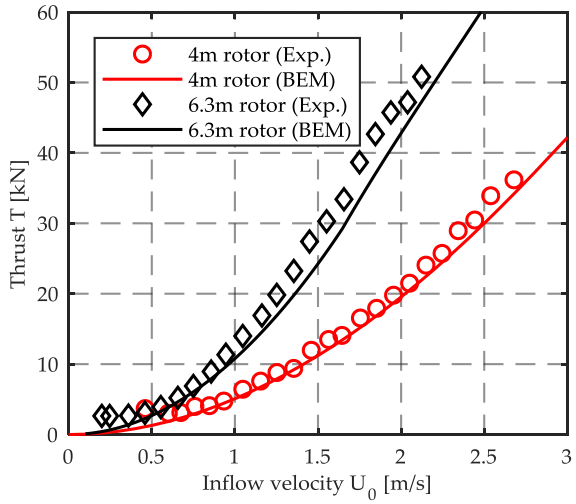

Fig. 14 Comparison of predicted and measured turbine thrust as function of the inflow velocity for the 4 m rotor and the 6.3 m rotor

The C_P-C_T ratio is presented in Fig. 15 as function of the inflow velocity for both rotor sizes. For the operation at the optimal point (cp. Fig. 16) the 6.3 m rotor provides a significantly higher C_P-C_T ratio which confirms the results of the model scale tests. Furthermore, the comparison displays the progress of blade design from the 4 m to the 6.3 m design. Due to the overspeed control philisophy for $U_0 \geq 1.7$ m/s the C_P-C_T ratios are reduced for the 6.3 m rotor The agreement with the BEM predictions is very good for $U_0 \geq 1.2$ m/s.

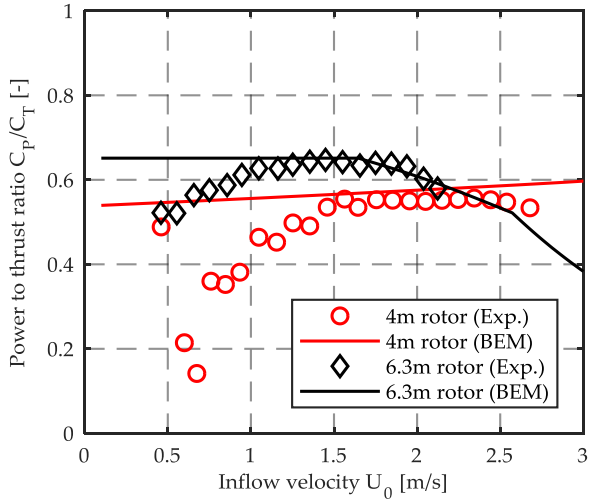

Fig. 15 Comparison of predicted and measured CP-CT ratio as function of the inflow velocity for the 4 m rotor and the 6.3 m rotor, respectively.

Fig. 16 shows the operating point of the turbine in terms of the tip speed ratio. Despite the turbulent flow conditions the controler is able to operate the turbine close to the respective optimum point, i.e. $\lambda = \lambda_{opt} = 5$ for the 4 m and $\lambda = \lambda_{opt} = 6$ for the 6.3 m rotor, respectively. To limit the turbine torque, the turbine with the 6.3 m rotor is operated at $\lambda \geq \lambda_{opt}$ for $U_0 \geq 1.7$ m/s ("overspeed").

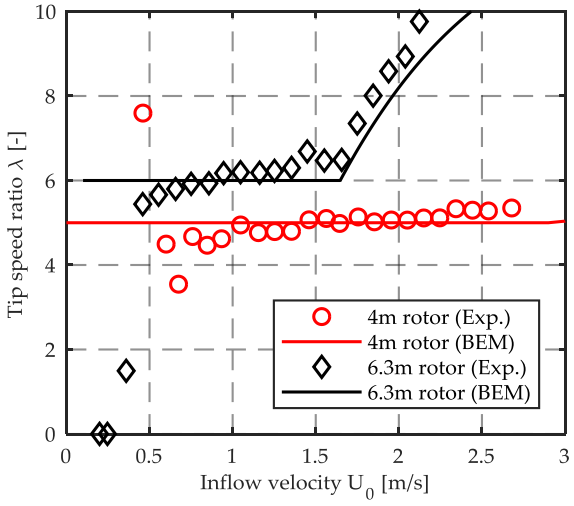

Fig. 16 Comparison of predicted and measured tip speed ratio as function of the inflow velocity for the 4 m rotor and the 6.3 m rotor

VI. CONCLUSION

The objective of this work was to present the experimentally obtained turbine performance characteristic for two different rotors of 4 m and 6.3 m diameter, respectively. Comprehensive model scale tests were conducted in a towing tank to determine no dimensional power and thrust characteristics of both designs. In the next step, both rotor designs were built in full-scale and mounted to the same drive train, resulting in two versions of SCHOTTEL HYDRO's fixed-pitch turbine SIT 250. The two turbine versions were deployed from the surface floating platform PLAT-I by Sustainable Marine Energy and tested at two different deployment sites. Post processing according to IEC 62600-200 has been used to evaluate the individual turbine performance.

The comparison of the results, model and full-scale, shows that the latest design, i.e. 6.3 m rotor, provides a favourable power to thrust ratio. However, the performance for both rotors shows good agreement with semi-empirical predictions using BEM. In general, the results derived from the testing provide a high level of design confidence.

The presented results represent important steps towards the commercialization of a turbine family. With this - now proven technology - the number of feasible deployments sites is significantly increased by solely adapting the rotor size to the local resource.

ACKNOWLEDGEMENT

This work been funded by the Federal Ministry for Economic Affairs and Energy of Germany (BMWi) in the project TIDAL POWER (FKZ 0325817B).

REFERENCES

[1] Wei Li, Hongbin Zhou, Hongwei Liu, Yonggang Lin, Quankun Xu, Review on the blade design technologies of tidal current turbine, Renewable and Sustainable Energy Reviews, Volume 63, 2016,p. 414-422.

[2] SIMEC Atlantis Energy, AR1500 Tidal Turbine. [Online] Available: https://simecatlantis.com/wp/wp-content/uploads/2016/08/AR1500-Brochure-Final-1.pdf. Accessed on: 10-January-2019.

[3] R. Starzmann, M. Baldus, E. Groh, N. Hirsch, N.A. Lange, S. Scholl, A Stepwise approach towards the development and full-scale testing of a marine hydrokinetic turbine, Proceedings of the 1st Marine Energy Technology Symposium (METS13), April 10-11, 2013, Washington, D.C.

[4] D. Sale, J. Jonkman, W. Musial, "Hydrodynamic Optimization Method and Design Code for Stall-Regulated Hydrokinetic Turbine Rotors". in *Proc. ASME 28th International Conference on Ocean, Offshore, and Arctic Engineering,* Honolulu, Hawaii.31 May to 5 June 2009

[5] M. Arnold, F. Biskup, and P. W. Cheng, "Load reduction potential of variable speed control approaches for fixed pitch tidal current turbines," International Journal of Marine Energy, vol. 15, pp. 175–190, 2016.

[6] Kaufmann, N., Carolus, T., Starzmann, R.; Multi-Objective Optimization of Blades for Fixed Pitch Horizontal Axis Tidal Stream Turbines with Variable Speed Control, In Proc. 12th European Wave and Tidal Energy Conference, Cork, Ireland, August 2017.

[7] Batten, W., Bahaj, A. S., Molland, A. F., Chaplin, J. R.: "The prediction of the hydrodynamic performance of marine current turbines". *Renewable Energy* vol. 33, Iss. 5, pp. 1085–1096, May 2008

[8] Masters, I., Chapman, J. C., Wilis, M. R., Orme, J.: "A Robust Blade Element Momentum Theory Model for Tidal Stream Turbines Including Tip and Hub Loss Corrections". *Journal of Marine Engineering and Technology,* vol. 10, Iss.1, pp. 25–35, Jan. 2011

[9] N. Kaufmann, T. H. Carolus, R. Starzmann, "An Enhanced and Validated Performance and Cavitation Prediction Model for Horizontal Axis Tidal Turbines," International Journal of Marine Energy, submitted 2016.

[10] A. Ruopp, A. Ruprecht, and S. Riedelbauch, Automatic Blade Optimisation of Tidal Current Turbines Using OpenFOAM, In Proc. 9th European Wave and Tidal Energy Conference, Southampton, UK, 2011.

[11] A. Bahaj, A. Molland, J. Chaplin und W. Batten, „Power and thrust measurements of marine current turbines under various hydrodynamic flow conditions in a cavitation tunnel and a towing tank," Renewable Energy, Volume 32, Issue 3, pp. 407-426, March 2007.

[12] D. Wang, M. Atlar and R. Sampson, „An experimental investigation on cavitation, noise, and slipstream characteristics of ocean stream turbines," Proceedings of The Institution of Mechanical Engineers Part A: Journal of Power and Energy, Volume 221, Issue 2, pp. 219--231, 2007.

[13] Z. Sarichloo, F. Salvatore, F. Di Felice, M. Costanzo, R. Starzmann, C. Frost: Computational analysis and experimental verification of a Boundary Integral Equation Model for tidal turbines, In Proc. RENEW 2018, Lisbon, October 2018.

[14] Marine energy – Wave, tidal and other water current converters –Part 202: Scale testing of tidal stream energy systems IEC/TS 62600-202 ED1.

[15] ITTC 7.5-02-07-03.9, Recommended Guideline: Model Tests for Current Turbines , 2014.

[16] Marine energy – Wave, tidal and other water current converters – Part 200: Electricity producing tidal energy converters – Power performance assessment, IEC/TS 62600-200, 2014.

[17] J. McNaughton, S. Harper, R. Sinclair, and B. Sellar, "Measuring and modelling the power curve of a Commercial-Scale tidal turbine", In Proc. of 11th EWTEC, Nantes, France, 6-11 Sept 2015.

[18] P. Jeffcoate, R. Starzmann, B. Elsaesser, S. Scholl and S. Bischof, "Field Measurements of a Full Scale Tidal Turbine", International Journal of Marine Energy, Volume 12, pages 3-20, 2015.

[19] R. Starzmann, I. Goebel, P. Jeffcoate: Field Performance Testing of a Floating Tidal Energy Platform - Part 1: Power Performance, In Proc. 4th Asian Wave and Tidal Energy Conference, Taipee, 2018.

[20] R. Starzmann, M. Baldus, E. Groh, N. Hirsch and N. Lange, "Full-Scale Testing of a Tidal Energy Converter using a Tug Boat", In Proc. of 10th EWTEC, Aalborg, Denmark, 2-5 Sept 2013.

[21] R. Starzmann, P. Jeffcoate, S. Scholl, S. Bischof, and B. Elsaesser, "Field testing a full-scale tidal turbine Part 1: Power Performance Assessment", In Proc. of 11th EWTEC, Nantes, France, 6-11 Sept 2015.

[22] R. Starzmann, S. Bischof, S. Scholl, P. Jeffcoate, S. Molloy; Experimental investigations on model and full-scale characteristics of a hydrokinetic turbine; Proceedings of the 3rd Marine Energy Technology Symposium; 2015, Washington, D.C.

[23] (2002) ITTC-Recommended Procedures and Guidelines- testing and extrapolating methods, propulsion, cavitation, model-scale cavitation test, Available: http://ittc.info/media/1844/75-02-03-031.pdf. Accessed February 18, 2019.

[24] P. Jeffcoate, N. Cresswell, "Field Performance Testing of a Floating Tidal Energy Platform - Part 2: Load Performance", In Proc. 4th Asian Wave and Tidal Energy Conference, Taipee, 2018.

[25] J. McMillan, A. Hay, R. Karsten, G. Trowse, D. Schillinger and M. O'Flaherty-Sproul, "Comprehensive Tidal Energy Resource Assessment in the lower Bay of Fundy, Canada", In Proc. of 10th EWTEC, Aalborg, Denmark, 2-5 Sept 2013.

[26] R. Karsten and M. O'Flaherty-Sproul, "Numerical modelling of Digby Neck tidal currents," OERA, Tech. Rep., March 2013.

[27] A. Hay, R. Karsten, G. Trowse, D. Morin, T. Webster, J. McMillan, M. O#Flatherty-Sproul, D. Schillinger, R. Cheel, E. Marshall and N. Crowell, "Southwest Nova Scotia Tidal Resource Assessment", OERA Technichal . Report, June 2013.

[28] J. McMillan and A. Hay, "Spectral and structure function estimates of turbulence dissipation rates in a high-flow tidal channel using broadband ADCPs", J. Atmos. Oceanic Technol., 34, 5–20 doi:10.1175/JTECH-D-16-0131.1.

[29] R. Starzmann, S. Bischof; "Cavitation Observations of a Full- and Model-Scale Instream Turbine", In Proc. 12th European Wave and Tidal Energy Conference, Cork, Ireland, August 2017

[30] N. Kaufmann, "Small Horizontal Axis Free-Flow Turbines for Tidal Currents" PhD diss., University of Siegen, December 2018.